Computer Assisted Methods in Engineering and Science, **20**: 73–79, 2013.

TWENTY YEARS OF THE CAMES

Modelling dynamics of transmission conductors with Cosserat rod

Hui Xiong[1,2], Zheng-liang Li[1,2]
[1] *College of Civil Engineering, Chongqing University*
Chongqing, China
[2] *Key Laboratory of New Technology for Construction of Cities in Mountain Area*
Chongqing, China

Jian Chang, Lihua You, Jian J. Zhang
National Centre for Computer Animation, The Media School, Bournemouth University
Poole, UK

Meili Wang
College of Information Engineering, Northwest Agriculture & Forestry University
Yangling, Shaanxi, 712100, China
e-mail: meili_w@nwsuaf.edu.cn (corresponding author)

We proposed a method to analyze the galloping, a vibration by wind force, of transmission conductors. The Cosserat rod model was introduced to describe the motion of the conductor line. The deformation was tracked using the intrinsic framework of material coordinates which are able to handle the large motion in galloping phenomena. The Cosserat model provided a theory framework to simulate the non-linear coupling of the torsional motion and the translational motion. Such non-linear coupling was reported as one of the main causes for the galloping phenomena.

Keywords: galloping, numerical simulation, conductor, Cosserat rod.

1. Introduction

Galloping is known as a low frequency, large amplitude oscillation of overhead single or bundled electrical transmission lines when they are subject to wind force. Such a wind-induced oscillation is more likely to occur in severe weather condition if the ice or wet snow accretion on the conductor changes its cross-sectional shape such that it becomes aerodynamically and/or aeroelastically unstable [1]. Severe galloping may bring flashover between phases and cause fatigues and damages to the conductors, the support hardware and even the tower structures. In the extreme case, the dynamic loads can trigger cascading of the transmission line and collapsing of the tower.

Great efforts have been made to bring in-depth understanding of the mechanism of the galloping phenomena. The study by Den Hartog [2] in the early thirties suggested the aerodynamic instability was the main cause for the phenomenon and Den Hartog introduced a criterion based on the drag coefficient and the lift coefficient to describe the condition of galloping developing. Den Hartog's explanation was based on the simplification that the vertical motion of the conductor was dominant and the influence of torsional and horizontal motion could be negligible. Latter research studies [3–5] discovered that the torsional motion was an integral part of the galloping phenomena. The coupling effect of the torsional motion with the translational motion plays a central role in most

cases of galloping evolving. A conclusion was drawn that Den Hartog's explanation was suitable for the rare cases with reverse wind and that the self-excited torsional mechanism was probably the most common ground of galloping [6, 7].

The numerical analysis provides powerful tools to investigate into the phenomena, as is compliment to the field observation and in-house experiment. Lump mass model [8–10] was initially introduced to analyse the vibration of transmission line. With radical simplification, the conductor was represented with a collection of central mass points which were linked with each other by springs and damp elements. This model provided some insight into the complex phenomenon of fluid-structure interaction in conductor galloping. Recent numerical analysis [11–13] took the advantages of more powerful approaches such as finite element analysis and finite difference method, which were able to simulate the phenomenon with higher accuracy and provided more useful information.

Our study of the galloping benefited from a well-established mechanical model of the conductor line which is able to take into account the influence of shape changes and non-linear coupling of torsional and translational motions. Existing linear models are not sufficient to simulate the dynamics associated with this complex nature of the phenomena. In this paper, we introduced the Cosserat model [14], which is designed to model the complex non-linear behaviour of long thin slender structures. It is capable to capture the non-linear large deformation/motion with the attached reference framework and provide a full description to the coupling of various motions.

Recently, Bertails *et al.* [15] proved the efficiency of using the Cosserat rod to model the complex dynamics of long hair which is traditionally hard to simulate with other approaches. Chang et al. [16] applied the Cosserat rod to model biological tissues for virtual surgery applications and Pai [17] used it to compute the shape of a surgical wire in the simulation of surgery. Chang et al. [18] developed the mode analysis for the dynamics of Cosserat rod structure which can represent the vibration of complex geometry in an efficient manner. Based on the success of these previous implementations, we will develop a novel approach to formulate the complex dynamics of galloping phenomenon using the Cosserat rod model in the following sections.

2. Cosserat rod model

In order to capture the large deformation of the conductor in question, we introduced the Cosserat rod mechanics. The Cosserat rod model [14] was developed to describe the deformation of a long thin rob-like object. The studied object is modelled with a space curve where its cross section is represented as one single point on the curve with attached coordinate framework. In our application, such a curve is selected as the centroid curve of the conductor.

As shown in Fig. 1, a local coordinate frame is attached at each point on the curve to indicate the translation and rotation of the cross section. We define $\mathbf{r}(s)$ as a point on the selected curve, where s is the parameter defined by the curve length ranging from 0 to L. The coordinate frame at a given point can be denoted by three directional vectors (directors) $\mathbf{d}_1$, $\mathbf{d}_2$ and $\mathbf{d}_3$ which are orthogonal to each other. By convention, the director $\mathbf{d}_3$ is selected so to make it parallel to the tangent direction of the centroid curve.

$$\begin{aligned} &\mathbf{d}_3 \times \frac{\partial \mathbf{r}}{\partial s} = 0, \\ &\mathbf{d}_1 \times \mathbf{d}_2 = \mathbf{d}_3. \end{aligned} \tag{1}$$

The vertical motion and horizontal motion of a transmission conductor are recorded with the translation of a given material point $\mathbf{r}(s)$, which allows motion in three directions. In the mean time, the torsional motion can be defined with the rotation of the coordination frame along director $\mathbf{d}_3$. Six degrees of freedom are used to describe the kinemics of a cross-section of the transmission conductor. With such a treatment, the complicated case of coupling of different motions can be naturally formulated with consideration of non-linear effects of large deformation.

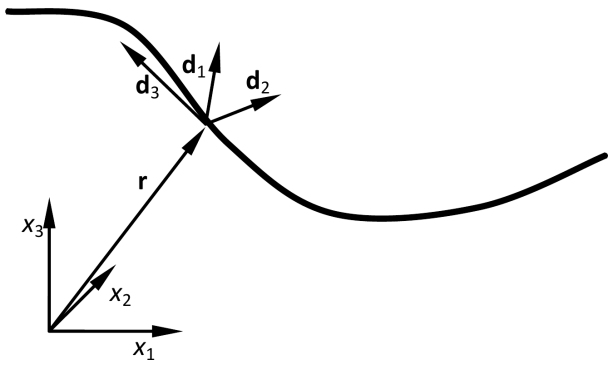

Fig. 1. Cosserat rod model.

The Darboux vector $\boldsymbol{\omega}$ is defined by the differential operation of the director along the curve as

$$\frac{\partial \mathbf{d}_i}{\partial s} = \omega \times \mathbf{d}_i, \quad \text{with} \quad i = 1, 2, 3. \tag{2}$$

With the Darboux vector, the twisting deformation is described with the torsion (τ) and the bending deformations are described with the flexures (κ_1, κ_2):

$$\boldsymbol{\omega} = \kappa_1 \mathbf{d}_1 + \kappa_2 \mathbf{d}_2 + \tau \mathbf{d}_3. \tag{3}$$

The derivative of the material point $\mathbf{r}(s)$ along the curve gives the measurement of deformation of shearing and extension.

$$\mathbf{v} = \frac{\partial \mathbf{r}}{\partial s} = v_1 \mathbf{d}_1 + v_2 \mathbf{d}_2 + v_3 \mathbf{d}_3, \tag{4}$$

where v_1 and v_2 denote the shear deformation of the cross section which is the tilting of the cross-section, and $(v_3 - 1)$ denotes the extension ratio which is the length change of the conductor line.

In the motion of transmission conductor, the shearing effect is negligible. We write the potential energy U of a given transmission conductor as follows,

$$U = \frac{1}{2} \int [B_1(\kappa_1 - \overline{\kappa}_1)^2 + B_2(\kappa_2 - \overline{\kappa}_2)^2 + GJ(\tau - \overline{\tau})^2 + EA(v_3 - 1)^2] ds, \tag{5}$$

where B_1 and B_2 are the associated bending stiffness coefficients, G is the shear modulus, J is the polar moment of inertia of the cross section, E is the Young's modulus and A is the area of cross section. In Eq. (5), the over bar ($^-$) denotes the quantities in the equilibrium state of the transmission conductor when no external loads are exerted. For the case of a small sag-span ratio, the bending items in the energy can be omitted and the Cosserat rod model degenerates to the cable model.

The equation of motion for the transmission line can be derived using the Hamilton's principle as suggested in [18]. We have

$$\int_{t_1}^{t_2} \delta(T - U) dt - \int_{t_1}^{t_2} \delta W dt = 0, \tag{6}$$

where T represents the kinetic energy, U represents the potential energy and W represents the virtual work by the external forces. The integration falls in the time interval from time t_1 to t_2. In Eq. (6), $\delta(\cdot)$ represents the variational operator with respect to virtual displacement.

$$T = \frac{1}{2} \int \rho A \frac{d\mathbf{r}}{dt} \cdot \frac{d\mathbf{r}}{dt} ds, \tag{7}$$

$$W = \int [\mathbf{f} \cdot (\mathbf{r} - \overline{\mathbf{r}}) + m(\theta - \overline{\theta})]ds. \tag{8}$$

In Eq. (7), ρ is the mass density of the transmission line and A is the cross-sectional area, the derivative of the position $\mathbf{r}$ with respect to time t represents the velocity vector. In Eq. (8), the external force $\mathbf{f}$ includes the gravity, the damping force and the aerodynamic drag and lift forces. The torque m is caused by the wind and θ records the twisting angle of a given section.

We can express the values on the continuous curve as interpolation of the values on discretized nodes. Using the variables defined on the discretized nodes and derived from Eq. (6), we reach the following control equation whose derivation can be found in [18].

$$M\ddot{\mathbf{q}}_k + C\dot{\mathbf{q}}_k + K\mathbf{q}_k = \mathbf{R}, \tag{9}$$

where $\mathbf{q}_k$ is the general displacement vector defined on node k which is related to the motion, $\dot{\mathbf{q}}_k$ is the general velocity and $\ddot{\mathbf{q}}_k$ is the general acceleration, M is the general mass matrix, C is the damping matrix, K is the stiffness matrix and R is the residual force.

3. Numerical results

The wind speed is random as shown in Fig. 2, which was simulated by a numerical model of stochastic process. In our computation, an average wind speed of 5.95 m/s was used.

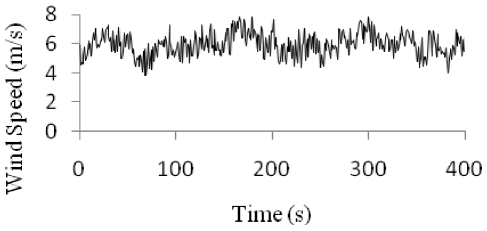

Fig. 2. Wind speed history.

The wind tunnel test was carried out to identify the aerodynamic characteristics for both single conductor and 8-bundled conductor. The test was conducted at China Aerodynamics Research and Development Center. A detailed report was included in [19]. It has been technically challenging to prepare a full scale wind tunnel test of transmission line galloping and this test was using samples with length of 180 mm. The aerodynamic drag coefficients: C_L (lift coefficient), C_D (drag coefficient), and C_M (pitch moment coefficient) with different attack angles, were measured in the test (an example of a single conductor is shown in Fig. 3).

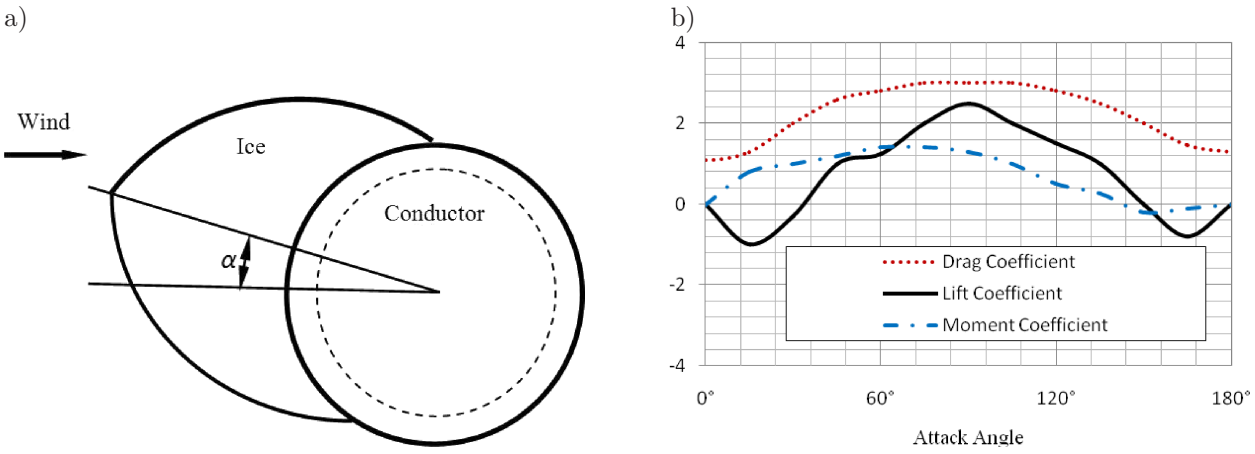

Fig. 3. (a) Ice shape and the definition of attack angle α, (b) aerodynamic coefficients versus attack angle.

We observed the measured dynamic coefficients in Fig. 3b were not symmetrical with respect to the attack angle of 90°. This was partly caused by the imperfection of the sample. And the more likely reason is that the shape of the accreted ice is not ideally symmetric. In the real cases, the ice shapes may vary, that can result in the different behaviours of the dynamic responding [19].

The conductor is represented as a collection of discrete segmentations in the discretized numerical model. The forces and torques at a segment of the Cosserat rod with respect to the wind speed can be computed out using the measured aerodynamic coefficients. Given the segment length as ΔL and its diameter as d, we have,

$$\mathbf{R} = \left\{ \begin{array}{c} f_1 \\ f_2 \\ f_3 \\ m \end{array} \right\} = \left\{ \begin{array}{c} \frac{1}{2} C_D \rho v^2 d \Delta L \\ \frac{1}{2} C_L \rho v^2 d \Delta L - f_g \\ 0 \\ \frac{1}{2} C_M \rho v^2 d^2 \Delta L \end{array} \right\}, \tag{10}$$

where ρ is the air density, v is the wind speed, and f_g is the gravity force.

Solving the discrete control Eq. (9) using the forces from Eq. (10), we are able to simulate the dynamics of a given conductor.

Figure 4 shows the motion of the centre of mid-span when the simulation started. It behaved stochastic and depended on the randomness of the input wind forces. However, if the wind direction did not flip over, such a motion converged to a stable galloping as shown in Fig. 5. The two figures show different stages when a galloping was developed.

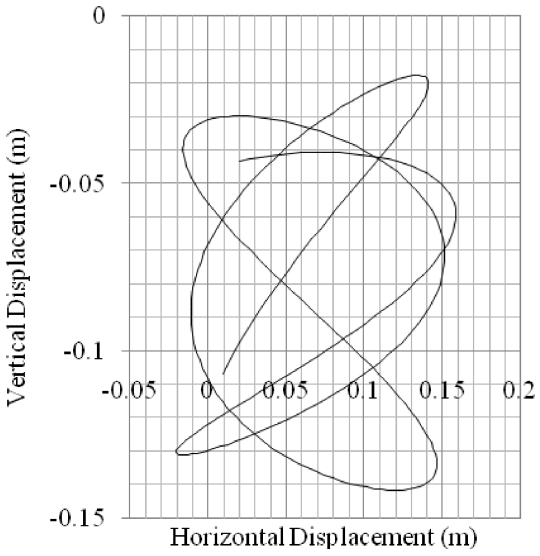

Fig. 4. Trace of the mid-span in the instable state.

When the wind force was initially applied, we observed stochastic motion (Fig. 4) of the conductor which directly reflected the change of the input force. If the wind force lasted and no sudden flipping over occured, the motion could be transferred into a stable oscillation (Fig. 5). That indicated the dynamic balance of the input energy and the dissipating energy. The motion of the conductor line followed a certain trajectory or a certain pattern of movement. If the wind force decreases or increases gradually, the trajectory could shrink or amplify.

In the stable case (Fig. 5), the dynamic system reached its balance, where the inputted energy equalled to the energy dissipation. The vibration amplitude of the vertical motion in Fig. 5 is larger than that of the instable motion in Fig. 4. It implies that the energy of horizontal motion

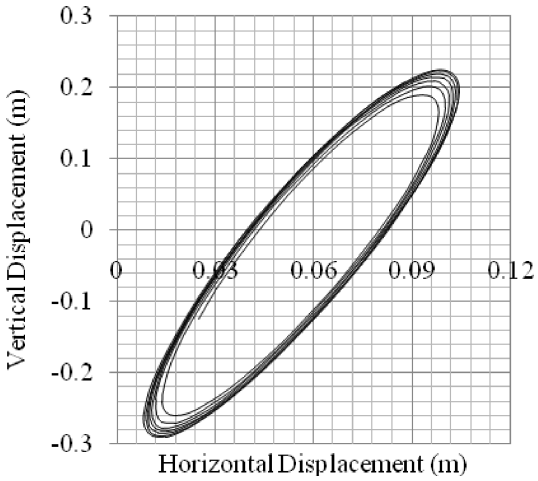

Fig. 5. Galloping trace of the mid-span in the stable state.

was transferred to the vertical motion via the torsional coupling. The amplitude of the oscillation increased with time until it reached a stable galloping state.

In our numerical experiment, if we defined a larger torsional stiffness GJ in Eq. (5), it was observed that the time required to reach stable galloping state became longer and the amplitude of vertical motion was smaller. It suggests that multi-bundled conductors can effectively reduce the risk of galloping with larger torsional stiffness.

4. Conclusions

Galloping as a wind-induced vibration of transmission line has been studied for many years to understand its complex mechanism. Accurate numerical models which simulate the phenomena can bring theoretical insight and suggest valid control approaches.

In this paper, we introduced a Cosserat rod model to describe the motion of a transmission line. The Cosserat rod took the advantages of describing the motion in a natural material frame which is suitable for computing large motion which is often the case when galloping occurs. It modelled the nonlinear coupling of torsional and translational movement.

When compared to other linear approaches, such as finite element method using cable elements, the computational speed of our approach was slower. The nonlinear feature of our model requires to updates the coefficients in the governing equations at run time. We have demonstrated two phases of motion in galloping formation: one is instable initial phase and the other is stable oscillation. The different patterns of motion were illustrated, which suggested possible energy redistribution in the dynamic system which resulted in the self-exited vibration.

In the near future, we will investigate the complexities of multi-bundled conductors by developing an extended Cosserat model to indicate how to optimise the parameters and bundle lay-out so to improve the aero-dynamic stability and reduce the potential damages caused by galloping phenomenon. Future research in this direction will bring more in-depth understanding of the galloping in both theoretical and practical applications.

Acknowledgement

This research is partly supported by National Natural Science Foundation of China (50678181, 50708118), the Fundamental Research Funds for the Central Universities of China (CDJZR1120001), the Fundamental Research Funds (ZD2012018) of Northwest A&F University.

References

[1] O. Chabart, J.L. Lilien. Galloping of electrical lines in wind tunnel facilities. *J. Wind Eng. Ind. Aerodyn.*, 74–76, 967–976. DOI: 10.1016/S0167-6105(98)00088-9, 1998.

[2] J.P. Den Hartog. Transmission line vibration due to sleet, *Trans. A.I.E.E.*, **51**(4): 1074-1076. 1932.

[3] O. Nigol, G.J. Clarke. Conductor galloping and control based on torsional mechanism. *IEEE. Power Eng. Soc. Winter Mtg.*, IEEE C-74016-2, 1974.

[4] K.G. McConnel, C.N. Chang. A study of the axial-torsional coupling effect on a sagged transmission line. *Exp Mech.*, 324–329, 1986.

[5] A. Luongo, D. Zulli, G. Piccardo. On the effect of twist angle on nonlinear galloping of suspended cables. *Comput. Struct.*, **87**(15–16): 1003–1014, 2009.

[6] O. Nigol, P.G. Buchan. Conductor galloping – part 1, Den Hartog mechanism. *IEEE. Power Eng. Soc. Summer Mtg.*, IEEE F-79714-7, 1979.

[7] O. Nigol, P.G. Buchan. Conductor galloping – part 2, torsional mechanism. *IEEE. Power Eng. Soc. Summer Mtg.*, IEEE F-79715-4, 1979.

[8] C.B. Rawlins. *Transmission Line Reference Book: Wind-Induced Conductor Motion*. Electrical Power Research Institute. Palo Alto, California, U.S.A. 1979.

[9] P. McComber, A. Paradis. A cable galloping model for thin ice accretions. *Atmos. Res.*, **46**(1–2): 13–25, DOI: 10.1016/S0169-8095(97)00047-1, 1998.

[10] D. Burton, D.Q. Cao, R.W. Tucker, C. Wang. On the stability of stay cables under light wind and rain conditions. *J. Sound Vib.*, **279**(1–2): 89–117, DOI: 10.1016/j.jsv.2003.10.038, 2005.

[11] Y.M. Desai, P. Yu, N. Popplewell, A.H. Shah. Finite element modelling of transmission line galloping. *Comput. Struct.*, **57**(3): 407–420, DOI: 10.1016/0045-7949(94)00630-L, 1995.

[12] Q. Zhang, N. Popplewell, A.H. Shah. Galloping of bundle conductor. *J. Sound Vib.*, **234**(1): 115–134, DOI: 10.1006/jsvi.1999.2858, 2000.

[13] X. Liu, B. Yan, H. Zhang, S. Zhou. Nonlinear numerical simulation method for galloping of iced conductor. *Appl. Math. Mech. – Engl. Ed.*, **30**(4): 489–501, 2009.

[14] S. Antman. *Applied Mathematical Sciences, 107 – Nonlinear Problems of Elasticity*. Springer Verlag, 1995.

[15] F. Bertails, B. Audoly, M. Cani, B. Querleux, F. Leroy, J. Lévêque. Super-helices for predicting the dynamics of natural hair. *SIGGRAPH'06*, 1180–1187, 2006.

[16] J. Chang, J. Pan, J.J. Zhang. Modelling rod-like flexible biological tissues for medical training. *LNCS 5903*, 51–61, 2009.

[17] D. Pai. Strands: interactive simulation of thin solids using Cosserat models. *Comput. Graph. Forum*, **21**(3): 347–352, 2002

[18] J. Chang, D.X. Shepherd, J.J. Zhang. Cosserat-beam-based dynamic response modelling. *Comput. Animat. Virtual Worlds*, **18**(4–5): 429–436, DOI: 10.1002/cav.v18:4/5, 2007.

[19] Z. Xiao, Z. Yan, Z. Li, Z. Wang, H. Huang. Wind tunnel and aerodynamic characteristics tests for ice-covering of transmission line adopting 8-bundled conductor. Power Sys. Tech., **33**(5): 90–94, 2009.